

COUNTING EQUILIBRIA OF THE ELECTROSTATIC POTENTIAL

HERBERT EDELSBRUNNER, CHRISTOPHER FILLMORE, AND GONÇALO OLIVEIRA

ABSTRACT. A century and a half ago, James C. Maxwell [7] conjectured that the number of zeroes of the electric field (equilibria of the potential) generated by a collection of n point charges is at most $(n - 1)^2$. In 2007 Gabrielov, Novikov and Shapiro proved a much larger upper bound and posed two further conjectures [6]. It is quite possible that Maxwell’s quadratic upper bound is not tight, so it is prudent to find lower bounds. Our main contributions in this article are:

- the construction of examples that achieve the highest ratios of number of electric field zeroes by point charges found to this day;
- a counterexample to Conjecture 1.8 in [6] that the number of equilibria cannot exceed those of the distance function defined by the unit point charges.

1. INTRODUCTION

Context. Let A_1, A_2, \dots, A_n be points in \mathbb{R}^3 with corresponding real charges $\zeta_1, \zeta_2, \dots, \zeta_n$. We call A_i together with ζ_i a *point charge*. The *electrostatic potential* generated by the n point charges is the function $V: \mathbb{R}^3 \setminus \{A_1, A_2, \dots, A_n\} \rightarrow \mathbb{R}$ defined by

$$(1) \quad V(x) = \sum_{i=1}^n \frac{\zeta_i}{\|x - A_i\|},$$

in which $\|x - A_i\|$ is the Euclidean distance between the two points. The *electric field* is the gradient of this potential. In this article, we shall focus in the case in which all the charges ζ_i are positive. The zeros of the electric field are the *equilibria* or the *critical points* of the potential. They are also sometimes referred to as *electrostatic points* as they are the points at which the electric field vanishes, thus corresponding to equilibrium positions for test charges.

A well-known Morse theoretic argument reviewed later in Section 2, shows that, for the generic location of n point charges, the number of equilibria is at least $n - 1$. For example, this is achieved by placing the point charges along a line. One may wonder which configurations of charges generate the maximum number of equilibria. This is at the core of the 1873 conjecture posed by Maxwell in his famous “A Treatise on Electricity and Magnetism”.

Conjecture 1 (Maxwell in [7]). *The electrostatic potential defined by n point charges in \mathbb{R}^3 has at most $(n - 1)^2$ equilibria.*

For $n = 3$, this conjectured upper bound is attained by the vertices of an equilateral triangle in \mathbb{R}^3 . Placing a unit charge at each of these three points, we get three 2-saddles and one 1-saddle, so a total of four equilibria of V .

A general upper bound on the number of equilibria was only obtained in 2013 [6]. However, it grows much faster than the quadratic upper bound conjectured by Maxwell. Indeed, already for

Key words and phrases. Electric field, electrostatic potential, Morse theory, equilibria, Voronoi tessellations, counting.

$n = 3$ this bound is 139314069504. Beyond the upper bound, Gabrielov, Novikov and Shapiro prove interesting results and pose stimulating conjectures, which we will now explain and later address in this article. An important auxiliary tool in [6] is the family of potentials

$$(2) \quad V_p(x) = \sum_{i=1}^n \frac{\zeta_i^p}{\|x - A_i\|^p}, \quad \text{which satisfies} \quad \lim_{p \rightarrow \infty} \frac{1}{p\sqrt{V_p(x)}} = \min_{1 \leq i \leq n} \frac{\|x - A_i\|}{\zeta_i}.$$

The authors prove in Theorem 1.7 of that reference that for sufficiently large p , the number of equilibria of V_p of any given index remains constant with increasing p .¹ Then, for $j \in \{0, 1, 2, 3\}$, let $\#_j$ denote this limiting number of equilibria of V_p for $p \gg 1$. This result, plus the expectation that the number of equilibria of V_p is non-decreasing with p , for all $p \geq 1$ leads to the following conjecture.

Conjecture 2 (Conjecture 1.8 (a) in [6]). *For n unit point charges in generic position, and all $p \geq 1$, the number of index j equilibria of V_p is at most $\#_j$.*

As we shall see later in this introduction, we will provide a counterexample to this conjecture. On the other hand, for even p , one can easily obtain a linear upper bound on the number of equilibria of the restriction of V_p to any line in Euclidean space. A stronger version of this statement was also conjectured in [6] as we shall now state.

Conjecture 3 (Conjecture 1.9 in [6]). *For all $p \geq 1$, the number of equilibria of the restriction of V_p to any straight line in \mathbb{R}^3 is at most $2n - 1$.*

Main Results. As stated in the abstract, the key contributions of this article are a new record for the ratio of the number of equilibria over the number of point charges, a counterexample to Conjecture 2, and a number of other interesting results and explorations. In Sections 2, we give a general discussion and exploration of examples obtained by placing unit charges at the vertices of several polyhedra. It is here that we arrive at our first main result, which is a family of examples constructed in Sections 2.3 and 2.4. The conclusion of that construction is the following.

Result 1 (New record for number of equilibria). *For any $\varepsilon > 0$, there are a sufficiently large integer, n , and point charges, $\{A_1, A_2, \dots, A_n\} \subseteq \mathbb{R}^3$, such that*

$$(3) \quad V(x) = \sum_{i=1}^n \frac{1}{\|x - A_i\|},$$

has k equilibria with $\frac{k}{n} > \frac{25}{7} - \varepsilon$.

Our construction gives a precise family of examples which, for each $\ell \in \mathbb{N}$ constructs a configuration of $n_\ell = 8^\ell$ points with unit charges in \mathbb{R}^3 that define an electrostatic potential with $\frac{25}{7}(n_\ell - 1)$ equilibria. Recently, there has been interest in constructing closed geodesics on Calabi-Yau manifolds [4], and this result may find applications to that purpose [12].

¹In fact, said theorem proves that for sufficiently large p , the equilibria of V_p are in correspondence with the so-called effective cells of positive codimension in the corresponding Voronoi diagram. Furthermore, the Morse index of such equilibria coincides with the dimension of the corresponding cell.

In Section 3, we study the potentials V_p defined in (2) and, after deducing some results, culminate with our second main result which is a counterexample to [6, Conjecture 1.8(a)]. The conclusion of the discussion in Section 3.2 can be summarised as follows.

Result 2 (Counterexample to Conjecture 2). *Let A_1 to A_{24} be the unit point charges at the vertices of the truncated octahedron—the Voronoi domain in the body centered cubic lattice—and consider the resulting 1-parameter family of potentials*

$$(4) \quad V_p(x) = \sum_{i=1}^n \frac{1}{\|x - A_i\|^p}.$$

Then, there is p_ such the number of index-1 equilibria of $V = V_1$ is greater than that of V_p for all $p > p_*$; that is: greater than $\#_1$.*

In the above counterexample, the number of index-2 equilibria is equal to $\#_2$, so even the total number of equilibria of V is larger than that of the limiting Euclidean distance function.

In addition to the main results, this article contains a number of other contributions, including a thorough exploration of the electrostatic potential generated by unit point charges positioned at the vertices of several interesting convex polyhedra. For example, we observe the following curious phenomenon: the configurations obtained by placing the unit charges at the vertices of Platonic and Catalan polyhedra never generate electric potentials with 1-saddles, while for Archimedean polyhedra—which are dual to the Catalan ones—such 1-saddles are always present. We also observe, for even p , the upper bound of $p(n - 1) + 2n - 1$ on the number of equilibria of the restriction of V_p defined by n unit point charges to any line in \mathbb{R}^3 .

2. REGULAR CONFIGURATIONS

This section starts out by using Morse theory to show that for non-degenerate potentials generated by n unit point charges in \mathbb{R}^3 , there are at least $n - 1$ equilibria. There are however configurations with more than $n - 1$ equilibria, and as mentioned in the introduction, the quadratic upper bound $(n - 1)^2$ was conjectured by Maxwell [7]. This bound is realised for $n = 3$, for example when placing charges at the vertices of an equilateral triangle. However, configurations that achieve this bound are not known for $n > 3$, and numerical experiments suggest that for randomly placed charges the ratio of the number of equilibria over point charges is bounded and rather low. Therefore, we shall now study special configurations of point charges, such as those obtained by placing them at the vertices of certain solids. This study leads in Section 2.3 to our first main result.

2.1. Morse Theory Considerations. An equilibrium of a smooth function is *non-degenerate* if the Hessian at the point is invertible. A useful result of Morse–Cairns in [10] yields that for the generic location of a single point charge, all equilibria of V are non-degenerate. In this case, the Hessian has 0, 1, 2, or 3 negative eigenvalues, and in Morse theory, this number is called the *index*; see e.g. [9]. Equilibria of index 0, 1, 2, 3 are referred to as *minima*, *1-saddles*, *2-saddles*, and *maxima*. Importantly, the electrostatic potential in \mathbb{R}^3 is *harmonic*; that is: its Laplacian vanishes at every point. To explain, it is not difficult to check that the Laplacian of the function $x \mapsto 1/\|x\|$ is harmonic on $\mathbb{R}^3 \setminus \{0\}$. Sums, translates, and multiples of harmonic functions are again harmonic,

which implies that V is harmonic. It follows that V enjoys the *mean value property*: $V(x)$ is the average of the values of V on any sphere centered at x that neither passes through nor encloses any of the A_i . Hence, if nonzero, V has neither minima nor maxima in $\mathbb{R}^3 \setminus \{A_1, A_2, \dots, A_n\}$.

An early application of Morse theory—carried out by Morse himself [10]—gives a lower bound on the number of equilibria of V . We shall now describe this argument, and its outcome under the assumption that $\zeta_i > 0$ for $1 \leq i \leq n$ and that all the equilibria are non-degenerate (as mentioned above, this can be achieved by simply perturbing one of the point charges). Because $\mathbb{R}^3 \setminus \{A_1, A_2, \dots, A_n\}$ is not compact, it is convenient to modify V to get a Morse function, $M: \mathbb{S}^3 \rightarrow \mathbb{R}$, that is sufficiently similar to V as follows:

- (1) compactify \mathbb{R}^3 to \mathbb{S}^3 by adding a point at infinity and extend V by continuity, so it takes the value 0 and has a local minimum there;
- (2) for each $1 \leq i \leq n$, define M inside a sufficiently small neighbourhood of A_i such that A_i is a maximum and the only equilibrium of M in this neighbourhood;
- (3) let M coincide with V outside these neighbourhoods and at the point at infinity.

Let m_p be the number of index- p equilibria of M . After subtracting the one minimum at infinity and the n maxima at A_1 to A_n , we get $m_0 + m_1 + m_2 + m_3 - (n+1)$ as the number of equilibria of V . By the Euler–Poincaré relation, we have $m_0 - m_1 + m_2 - m_3 = 0$ because the Euler characteristic of \mathbb{S}^3 vanishes. By construction, $m_3 = n$ and $m_0 = 1$, which thus implies $m_2 - m_1 = n - 1$. Hence, the number of equilibria of V is

$$(5) \quad m_1 + m_2 = 2m_1 + n - 1 \geq n - 1.$$

This lower bound is tight since placing n point charges along a straight line in \mathbb{R}^3 defines a potential with only $n - 1$ equilibria, all of which are 2-saddles.

2.2. Platonic Solids and Local Homology. We consider the vertices of the Platonic solids and semi-regular polyhedra as potentially interesting point charge configurations. The numbers of equilibria given in Table 1 were first obtained by numerical computations and graphical investigations, in which we discovered that all equilibria are non-degenerate, except the center of the solid, which unfolds into two or more such equilibria. Through lengthy but straightforward computations and arguments, we were then able to rigorously show the existence of the claimed equilibria. As an example, we present the full proof for the case of the cube in Appendix A.

solid	f -vector	2-saddles	1-saddles	center
Tetrahedron	(4,6,4,1)	0	0	3
Cube	(8,12,6,1)	12	0	-5
Octahedron	(6,12,8,1)	0	0	5
Dodecahedron	(20,30,12,1)	30	0	-11
Icosahedron	(12,30,20,1)	0	0	11

TABLE 1. Numerical results for the electrostatic potential defined by placing the point charges at the vertices of the five Platonic solids. The first entry in each f -vector is the number of point charges. The next two columns give the number of observed 2- and 1-saddles. In each case, the center is a degenerate equilibrium, for which we give the alternating sum of ranks in local homology. In each case, the number vertices exceeds this alternating sum plus the number of 2-saddles minus the number of 1-saddles by 1.

We use the local homology at a point to determine whether it is an equilibrium or not. For $x \in \mathbb{R}^3 \setminus \{A_0, A_1, \dots, A_n\}$, let $\varepsilon > 0$ be smaller than the distance between x and any of the n point charges, and write $B(x, \varepsilon)$ and $S(x, \varepsilon)$ for the closed ball and sphere with center x and radius ε . The *local homology* of V at x is the limit, for ε going to zero, of the relative homology of the pair $(B^-(x, \varepsilon), S^-(x, \varepsilon))$, in which $B^-(x, \varepsilon) \subseteq B(x, \varepsilon)$ and $S^-(x, \varepsilon) \subseteq S(x, \varepsilon)$ are the subsets of points y with $V(y) \leq V(x)$. To visually represent these groups, we define a binary function on the unit sphere, which maps $u \in \mathbb{S}^2$ to *black* if $V(x) < V(x + \varepsilon u)$, and to *white* if $V(x) \geq V(x + \varepsilon u)$ for every sufficiently small $\varepsilon > 0$. In words, the potential increases if we leave x in a black direction, and it decreases or stays the same if we leave x in a white direction; see the upper row in Figure 1 for the binary functions of a non-critical point and the four types of non-degenerate equilibria. Writing



FIGURE 1. *Upper row, from left to right:* the binary functions on the unit 2-sphere for a non-critical point, a minimum, a 1-saddle, a 2-saddle, and a maximum. *Lower row, from left to right:* the binary functions for the centers of the tetrahedron, cube, octahedron, dodecahedron, and icosahedron (these are degenerate equilibria and so are neither 1-saddles nor 2-saddles).

$W \subseteq \mathbb{S}^2$ for the white points, the local homology of x is the homology of the cone over W relative to W ; see the left and right halves of Table 2 for the ranks of these relative groups for the cases displayed in the first and second rows of Figure 1, respectively. For example, the rank vector of the tetrahedron is $(0, 0, 3, 0)$, which is consistent with three 2-saddles co-located at its center. It is also consistent with one minimum, four 1-saddles, and six 2-saddles co-located at the center, where the four 1-saddles cancel with the minimum and three of the 2-saddles. The latter choice is suggested by the face structure of the tetrahedron, which has one tetrahedron, four triangles, and six edges.

Observe that every geometric realization of the solid yields the same local homology. Indeed, a *similarity*—which is a map $\theta: \mathbb{R}^3 \rightarrow \mathbb{R}^3$ that is the composition of a scaling, a rotation, a translation, and possibly a reflection—preserves the types of equilibria. To prove this claim, we write $x' = \theta(x)$ and $V': \mathbb{R}^3 \setminus \{A'_1, A'_2, \dots, A'_n\} \rightarrow \mathbb{R}$ for the potential defined by the point A'_i with charges $\zeta'_i = \zeta_i$.

Lemma 1. *Let V, V' be the potentials defined by a finite set of point charges, before and after applying a similarity, respectively. Then there is a bijection between the equilibria of V and V' such that corresponding equilibria have the same type.*

	$p = 0$	1	2	3		$p = 0$	1	2	3
non-critical	0	0	0	0	tetrahedron	0	0	3	0
minimum	1	0	0	0	cube	0	5	0	0
1-saddle	0	1	0	0	octahedron	0	0	5	0
2-saddle	0	0	1	0	dodecahedron	0	11	0	0
maximum	0	0	0	1	icosahedron	0	0	11	0

TABLE 2. *Left half:* the ranks in local homology at the points whose binary functions are illustrated in the upper row of Figure 1. *Right half:* the ranks in local homology at the centers of the Platonic solids, with binary functions shown in the lower row of Figure 1. Observe that the last column in Table 1 is the alternating sum of these ranks.

Proof. A rotation, translation, and reflection does not change the value at a point, except that it transfers this value to the image of that point. This is not true for a scaling. Letting $s > 0$ be the scaling factor of the similarity, we have

$$(6) \quad V'(x') = \sum_i \frac{\zeta'_i}{\|x' - A'_i\|} = \sum_i \frac{\zeta_i}{s\|x - A_i\|} = \frac{1}{s}V(x),$$

at every $x \in \mathbb{R}^3$. Since multiplication with a positive constant preserves the local homology at a point, this establishes the claim for the bijection that maps an equilibrium to its image under the similarity. \square

2.3. Prisms and Anti-prism. Recall that the unit point charges at the vertices of the equilateral triangle in \mathbb{R}^3 define four equilibria, which implies that the ratio of equilibria over the number of vertices is $4/3$. Based on the numbers given in Table 1, we deduce that the corresponding ratios for the Platonic solids are $1/4$, $13/8$, $1/6$, $31/20$, and $1/12$, respectively, with the highest ratio for the cube (see also Appendix A for a proof of the existence of these equilibria). We get an even higher ratio of $33/12$ for the cuboctahedron; see the second row of Table 3. Indeed, this is the highest ratio we observe for the regular and semi-regular polytopes surveyed in Section 2.2 and Appendix B.

Beyond these families, we wish to consider the prisms and anti-prisms, which are parametrized by an integer, k , and a positive real number. A k -sided prism is the Cartesian product of a regular k -gon and an interval. It has two regular k -gons and k rectangles as facets. We call the aspect ratio of the rectangles the *relative height* of the prism. Lemma 1 applies only if two prisms agree on the k and on the relative height. Indeed, for the same k , the number of equilibria generated by unit point charges at the vertices of the prism depends on the relative height. We shed light on this dependence for the more interesting second family. A k -sided anti-prism has two regular k -gons in parallel planes as facets, one rotated relative to the other so that there are $2k$ isosceles triangles that connect the k -gons and complete the list of boundary facets; see Figure 2 for examples. The *relative height* of the anti-prism is the distance between the two k -gons over the length of their edges. Note that for $k = 3$ and the relative height chosen so that the isosceles triangles are equilateral, the 3-sided or triangular anti-prism is the (regular) octahedron.

Our experiments show that for $k \geq 4$, the relative height of the k -sided anti-prism can be chosen so that the electrostatic potential for unit point charges placed at the vertices has one 2-saddle for each edge, one 1-saddle for each isosceles triangle, and one additional 1-saddle at the center; see Figure 2 for illustrations and Appendix C for analytic proofs of some of these equilibria. For $k \geq 4$,

the ratio of equilibria over vertices is therefore

$$(7) \quad \frac{1}{2k}(4k + 2k + 1) = 3 + \frac{1}{2k},$$

For $k = 6$, this is the same ratio we get for the cuboctahedron after perturbing the point charges so that the degenerate equilibrium at the center unfolds into individual non-degenerate equilibria; see Section 2.4 for details. To maximize this ratio, we minimize the number of sides, which suggests that the 4-sided or square anti-prism is our best choice. In contrast, the equilibria for the 3-sided or triangular anti-prism are either too close to distinguish visually or are absorbed by a degenerate equilibrium at the center.

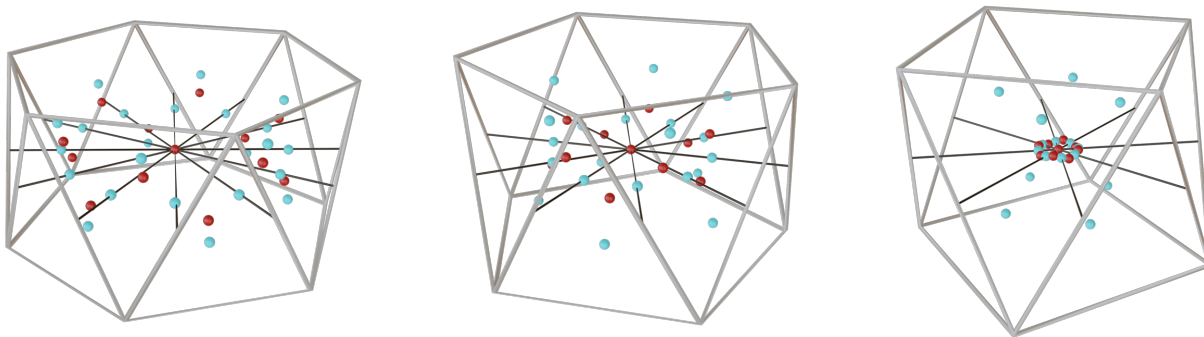


FIGURE 2. *From left to right:* the hexagonal, pentagonal, square anti-prisms with the heights chosen to maximize the number of equilibria. The ratios of equilibria over vertices are $37/12 < 31/10 < 25/8$, respectively. Observe how a ring of alternating 1- and 2-saddles gets successively more concentrated around the center.

In addition to the results on the maximum number of equilibria for anti-prisms, we discover an interesting universal phenomenon: the existence of a transition that occurs when the relative height of the prism or anti-prism is $\sqrt{2}$. This transition is universal in the sense that it occurs for both prisms and anti-prisms formed with any regular k -gon and always at relative height $\sqrt{2}$. We prove this in Appendix C and describe it here together with a result currently limited to the special cases of square and a triangular anti-prisms.

Theorem 1. *Consider the electrostatic potential generated by unit point charges at the vertices of any prism or anti-prism.*

- (1) *Its center is a non-degenerate equilibrium iff the relative height is not $\sqrt{2}$, in which case the center is a 1-saddle for relative heights less than $\sqrt{2}$ and a 2-saddle for relative heights larger than $\sqrt{2}$.*
- (2) *Moreover, if the relative height is larger than $\sqrt{2}$, there are two additional 1-saddles along the axis of the prism or anti-prism.*
- (3) *Furthermore assuming a square or triangular anti-prism and a relative height smaller than $\sqrt{2}$, there is an equilibrium on every line segment connecting the center of the anti-prism to the midpoint of a lateral edge.*

2.4. Increasing the Ratio. We can further increase the ratio in two steps. The first of these arises from the realization that the equilibrium at the center of a Platonic solid is necessarily degenerate and we can perturb the location of the charges so that it unfolds into several non-degenerate ones. Indeed, by Theorem 6.3 in [10], the point charges can be perturbed such that all equilibria are non-degenerate and arbitrarily close to the degenerate equilibria that give rise to them. Setting $N = m_1 - m_2 + n - 1$, we note that this is the alternating sum of local homology ranks at the center. It is also a lower bound for the number of 1-saddles and 2-saddles the degenerate equilibrium unfolds into. For example, we get three 2-saddles near the center of the tetrahedron, five 1-saddles near the center of the cube, and so on. Perturbing the vertices of the five Platonic solid thus increases the ratios to $3/4$, $17/8$, $5/6$, $41/20$, and $11/12$, respectively. Perturbing the vertices of the cuboctahedron increases the ratio to $37/12$. Compare this with the ratios $37/12 < 31/10 < 25/8$ for the hexagonal, pentagonal, square anti-prisms displayed in Figure 2, which are obtained without any perturbation.

In the second step, we iteratively substitute the vertices of a much smaller copy of the solid for each vertex of the original solid. Iterating $\ell - 1$ times, we get a configuration with ℓ layers. Letting n be the number of vertices of the solid and m the number of equilibria defined by these n charges, the number of point charges in the ℓ layers is $n_\ell = n^\ell$, and the number of equilibria is

$$(8) \quad m \cdot \left(n^{\ell-1} + n^{\ell-2} + \dots + 1 \right) = m \cdot \frac{n^\ell - 1}{n - 1} = \frac{m}{n - 1} \cdot (n_\ell - 1).$$

In particular, the ratio of the number of equilibria by electric charges in the ℓ -th iteration is given by $\frac{m}{n-1} \cdot \frac{n_\ell-1}{n_\ell}$, which for $\ell = 1$ coincides with the initial ratio of $\frac{m}{n}$, and as $\ell \rightarrow +\infty$ converges to $\frac{m}{n-1}$. In all examples we have computed, the iterated square anti-prism achieves the largest fraction $25/7$ in the limit, when $\ell \rightarrow \infty$. This is the highest ratio ever observed by far. In particular, we find that for any $\varepsilon > 0$, there is an iteration ℓ_* such that all further iterations $\ell > \ell_*$ have a ratio greater than $25/7 - \varepsilon$. This establishes Result 1 and naturally leads to the question of whether one can find an example of a configuration which achieves a greater ratio. We state this inquiry as follows.

Question. Can one find an example of a configuration of n unit point charges in \mathbb{R}^3 whose electrostatic potential has a number of equilibria that exceeds $25n/7$?

3. 1-PARAMETER FAMILY OF POTENTIALS

In the same way as in [6], we generalize the set-up by introducing a real parameter, $p > 0$, which modifies the effect of the distance to the point charges on the potential function:

$$(9) \quad V_p(x) = \sum_{i=1}^n \left(\frac{\zeta_i}{\|x - A_i\|} \right)^p.$$

Comparing (9) with (1), we see that $V = V_1$. The main purpose of this 1-parameter family of functions is to interpolate between the electrostatic potential and the (weighted) Euclidean distance function. The latter is the limit of one over the p -th root of V_p , as p goes to infinity:

$$(10) \quad E(x) = \lim_{p \rightarrow \infty} \frac{1}{\sqrt[p]{V_p(x)}} = \lim_{p \rightarrow \infty} \left(\sum_{i=1}^n \frac{\zeta_i^p}{\|x - A_i\|^p} \right)^{-1/p} = \min_{1 \leq i \leq n} \frac{\|x - A_i\|}{\zeta_i}.$$

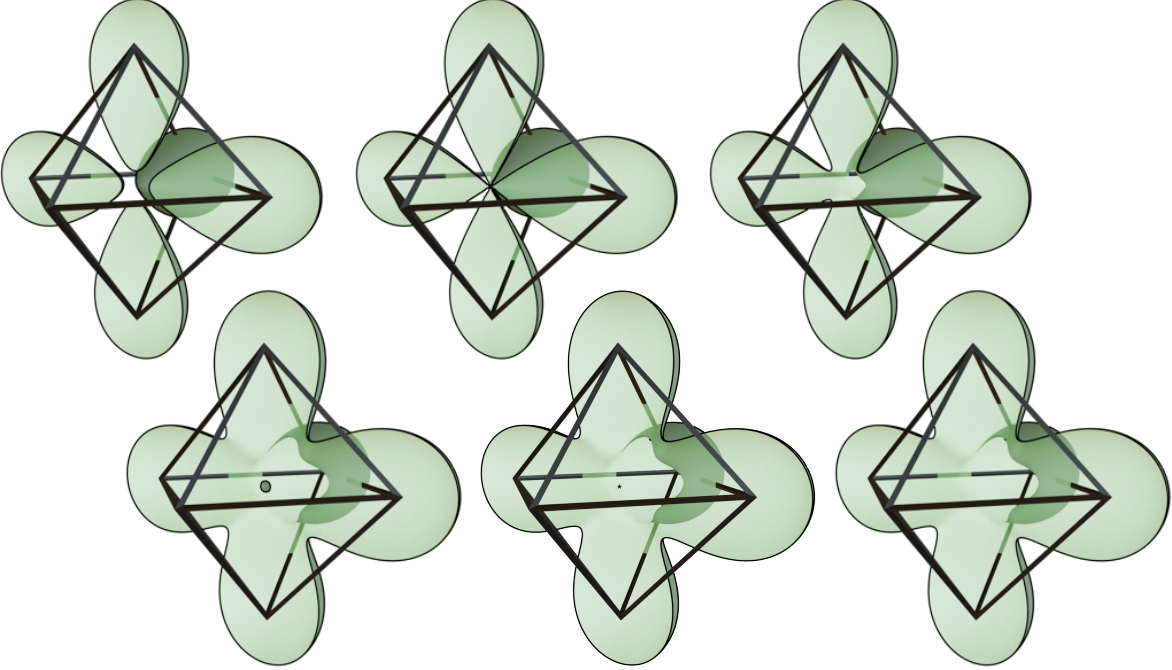


FIGURE 3. Cut-away views of three level sets of V_1 (upper row) and three level sets of $V_{1.3}$ (lower row) defined by point sources at the vertices of the octahedron. From left to right: the values are chosen slightly less than, equal to, and slightly greater than the potential at the center of the octahedron. Removing the front of the surface reveals some of the complication at the center, which for V_1 is a degenerate equilibrium; compare with Figure 1, but for $V_{1.3}$ is a minimum with a single point in the level set at the center.

3.1. No Maxima. For $p = 1$, V_p is harmonic and therefore has neither minima nor maxima. A weaker property still holds for more general values of p . Specifically, if $p \geq 1$ and all charges are positive, then V_p does not have any maxima:

Proposition 1. *Let $V_p: \mathbb{R}^3 \setminus \{A_1, A_2, \dots, A_n\} \rightarrow \mathbb{R}$ as defined in (9), and assume $\zeta_i > 0$ for every $1 \leq i \leq n$. Then for every $p \geq 1$, V_p has no maximum.*

We present the proof in Appendix D and illustrate the difference between the cases $p = 1$ and $p > 1$ in Figure 3, which shows a few level sets of V_1 and $V_{1.3}$. The tiny sphere around the center of the octahedron in the lower left level set suggests that the center is a genuine minimum of $V_{1.3}$, which it cannot be if $p = 1$ since this would contradict the harmonicity of V_1 . In fact, we can prove the following result showing that for $p > 1$, the origin is indeed a local minimum of the potential.

Proposition 2. *Let $\{A_1, A_2, \dots, A_6\}$ be the vertices of an octahedron and for $p \geq 1$*

$$V_p(x) = \sum_{i=1}^6 \frac{1}{\|x - A_i\|^p}.$$

Then, the center of the octahedron is a local minimum of V_p for all $p > 1$.

Again, the proof of this result will be presented in Appendix D. Finally, we point out that in this and other examples, the origin becomes a non-degenerate equilibrium for $p > 1$. Thus, in terms of

non-degeneracy, increasing the power, p , can have a similar effect as perturbing the point charges; see [10, Thm 6.3].

3.2. Counterexample. For positive and equal charges, the function $E: \mathbb{R}^3 \rightarrow \mathbb{R}$ defined in (10) is commonly referred to as the *Euclidean distance function* of the A_i and studied through the *Voronoi tessellation*, which assigns to each A_i the region of points that are at least as close to A_i as to any of the other points. If the charges are not necessarily the same (but still positive), then $E: \mathbb{R}^3 \rightarrow \mathbb{R}$ is a weighted version of the Euclidean distance function, namely with multiplicative weights $1/\zeta_i$. The corresponding tessellation of \mathbb{R}^3 is the *multiplicatively weighted Voronoi tessellation* [1, 11]. Both types of tessellations are described in more detail in Section 4.

The hope expressed as Conjecture 1.8 in [6]—and stated as Conjecture 2 in this article—is that $V: \mathbb{R}^3 \rightarrow \mathbb{R}$ cannot have more equilibria than $E: \mathbb{R}^3 \rightarrow \mathbb{R}$, in which the latter are defined using the limit process in (10). As stated in Result 2, the unit point charges at the vertices of the truncated octahedron form a counterexample to this conjecture, and we shall now explain why. This Voronoi domain is also known as the truncated octahedron; see Figure 4, which also shows the equilibria of the electrostatic potential defined by placing unit point charges at its vertices. This polytope has 14 faces (6 squares and 8 hexagons) and 36 edges (24 shared by a square and a hexagon and 12 shared by two hexagons). Correspondingly, E has 14 1-saddles and 36 2-saddles, which we compare to the 18 1-saddles and 36 2-saddles of V . Hence, the Euclidean distance function has fewer 1-saddles than the electrostatic potential of the same unit point charges, and it has equally many 2-saddles. In total, V has more equilibria than E , which contradicts Conjecture 1.8 in [6].

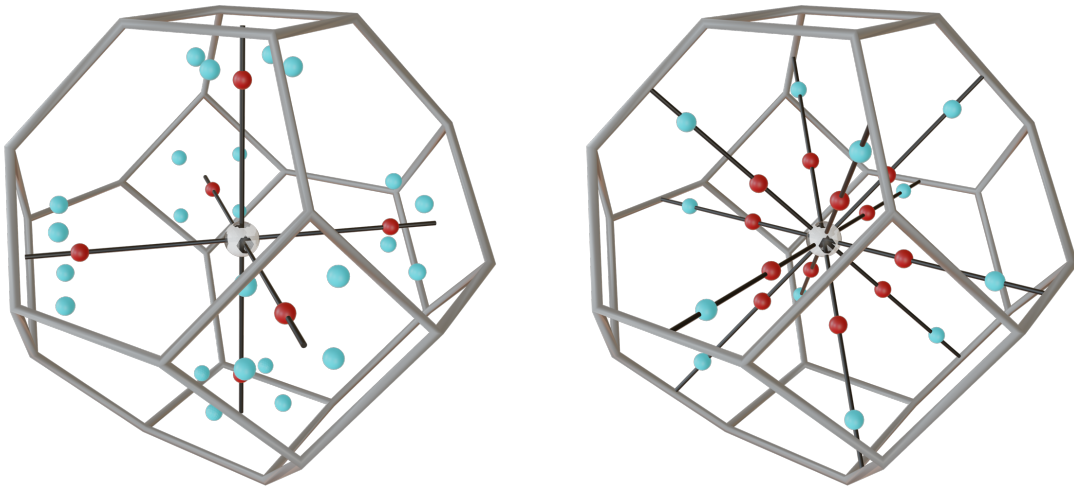


FIGURE 4. Equilibria of the electrostatic potential generated by unit point charges at the vertices of the truncated octahedron. In total there are 36 *light blue* 2-saddles, 18 *dark red* 1-saddles, and the degenerate equilibrium at the center. For better visualization, we split these equilibria into two groups, with one 1-saddle and four 2-saddles near each of the six squares displayed in the *left panel*, and one 1-saddle as well as one 2-saddle for each of the twelve edges shared by two hexagons in the *right panel*.

Making use of the obvious symmetries, we may associate equilibria of the electrostatic potential with the facets and edges of the polytope. For example, the line that passes through the centers

of two opposite squares is the intersection of four planes of symmetry, and it passes through three equilibria: the center and a 1-saddle near the square on either side. A more interesting example is the line that passes through the midpoints of two opposite edges shared by two hexagons each, which is the intersection of two planes of symmetry; see Figure 4. We observe that such a line passes through five equilibria: the center and two saddles on each side of the center. It is the only example we have so far, in which an edge of the polytope seems to be associated with more than one equilibrium. Furthermore, equilibria located along lines obtained as the common fixed locus of at least two reflections can be deduced to exist using the method implemented in Appendix A for the cube.

4. DISTANCE FUNCTIONS

Conjectures 1.8 and 1.9 in [6] motivate us to take a closer look at the Voronoi tessellations defined by the Euclidean distance function and its weighted version. The former relates to the case in which all points have equal charges, while the latter models the situation in which all charges are positive but not necessarily equal to each other.

4.1. Euclidean Distance. If the number of equilibria were monotonically non-decreasing with growing p , then the number of such points of V could be bounded from above by the number of such points of E . To study the latter, we introduce the *Voronoi domain* of A_i as the points $x \in \mathbb{R}^3$ that are at least as close to A_i as to any other A_j . This domain is a closed convex polyhedron, and the *Voronoi tessellation* is the collection of such domains, one for each point [13]. The intersection of any collection of Voronoi domains is either empty or a shared face, which we refer to as a *Voronoi cell*. The dual of the Voronoi tessellation is the *Delaunay mosaic* or *Delaunay triangulation* of the points [3]. It consists of convex polytopes that are convex hulls of subsets of the points. Specifically, the *Delaunay cell* that corresponds to a Voronoi cell is the convex hull of the points that generate the Voronoi domains sharing the Voronoi cell, and the Delaunay mosaic is the collection of Delaunay cells. Generically, the Delaunay mosaic is a simplicial complex, and in general it is a polyhedral complex.

Following [6], we call a Voronoi cell *effective* if its interior has a non-empty intersection with the interior of the corresponding Delaunay cell. Corresponding cells have complementary dimensions and lie in orthogonal affine subspaces, which implies that the intersection is either empty or a point. Effective cells are interesting because they are in bijection with the equilibria of E . Indeed, with increasing p , the equilibria tend toward the intersections of corresponding Voronoi and Delaunay cells; see Figure 5, which illustrates that already for $p = 2$ the equilibria are barely distinguishable from these intersection points. The Upperbound Theorem for convex polytopes [8] implies that the Voronoi tessellation of n points in \mathbb{R}^3 has at most $O(n^2)$ cells, and thus at most that many effective cells. Recently, [5, Theorem 3.1] proved that this bound is asymptotically tight:

Theorem 2. *For every $k \geq 2$, there exist $2k + 2$ points in \mathbb{R}^3 such that the Voronoi tessellation has $(k + 1)^2 - 1$ effective 1-dimensional and k^2 effective 2-dimensional cells.*

Does this lower bound translate to any meaningful lower bound for the electrostatic potential defined by the same number of points with equal charges? Perhaps not since the construction in [5]

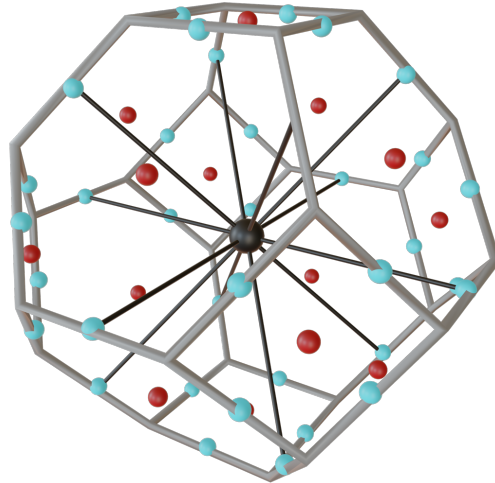


FIGURE 5. The equilibria of V_2 generated by unit point charges at the vertices of the truncated octahedron. Compared with V_1 , we note a drastically reduced number of 1-saddles and a minimum at the origin; see Figure 4 where we used two copies of the solid to show all equilibria. While $p = 2$ is still not large, the equilibria are already close to the barycenters of the facets and edges of the solid.

is delicate and the authors of this article have not been able to get a quadratic number of equilibria of V for similarly placed points.

4.2. Weighted Euclidean Distance. If we allow points with different charges, then E is the multiplicatively weighted Euclidean distance function; see (10). We can still define Voronoi domains, tessellation, and cells, but there are significant differences:

- a domain is no longer the common intersection of closed half-spaces but of $n - 1$ closed balls and closed complements of balls, and thus not necessarily connected;
- already in \mathbb{R}^2 , the tessellation may consist of $\Theta(n^2)$ vertices, (circular) edges, and (connected) regions [1];
- there is no established dual structure, like the Delaunay mosaic in the unweighted case.

In the plane, the maximum numbers of cells in the Voronoi tessellation differ even asymptotically between the unweighted and the weighted cases: $\Theta(n)$ versus $\Theta(n^2)$. In \mathbb{R}^3 on the other hand, the maximum number of cells is $\Theta(n^2)$ in both cases. There is at most one equilibrium of E per Voronoi cell, so we have at most $\Theta(n^2)$ such points. However, the difference in the maximum number of cells in \mathbb{R}^2 begs the question whether the maximum number of equilibria differ in the same way. We think not.

Conjecture 4. *The number of equilibria of the weighted Euclidean distance function defined by n points with positive real weights in \mathbb{R}^2 is at most some constant times n .*

The number of equilibria in the plane is relevant because they can be turned into higher index equilibria in three dimensions.

4.3. Slices. Consider the Voronoi tessellation that represents the weighted or unweighted Euclidean distance function defined by n weighted or unweighted points in \mathbb{R}^3 . We call the restriction to a

plane or a line a *slice*. These restrictions look a lot like the lower-dimensional tessellations, but they are more general and can be defined by adding a weight to the respective squared distance to the i -th point:

$$(11) \quad \pi_i(x) = \|x - A_i\|^2 + w_i;$$

$$(12) \quad \varphi_i(x) = \left(\frac{\|x - A_i\|}{\zeta_i} \right)^2 + w_i,$$

in which w_i is the squared distance of A_i from the plane or line. The weighted squared distance in (11) is known as *power* or *Laguerre distance*, and while it is a special case of (12), it received substantially more attention in the mathematical literature. In both cases, the 1-dimensional tessellation has at most $O(n)$ cells and thus at most that many equilibria.² This is also true for the 2-dimensional tessellation defined by the weighted squared distance in (11), but see Conjecture 4 to the more general weighted squared distance in (12). By reducing to the same denominator and appealing to the fundamental theorem of algebra, one obtains that, for even $p > 0$ and V_p defined by n unit point charges, its restriction to a straight line in \mathbb{R}^3 has at most $p(n-1) + 2n - 1$ equilibria. While we have no proof, we venture that this bound can be strengthened to at most $O(n)$ equilibria for any $p > 0$, and extended to 2-dimensional slices. To focus, we formulate a more restricted version:

Conjecture 5. *Let $V: \mathbb{R}^3 \setminus \{A_1, A_2, \dots, A_n\} \rightarrow \mathbb{R}$ be the electrostatic potential as in (1). Then the restriction of V to any straight line or flat plane in \mathbb{R}^3 has at most $O(n)$ equilibria.*

5. DISCUSSION

Inspired by the article of Gabrielov, Novikov and Shapiro [6], we studied the connection between the electrostatic potential and the (weighted) Euclidean distance function defined by a finite collection of point charges. We focus on the 3-dimensional case and on positive charges, which may or may not all be the same. We have three main results, the second of which is a counterexample to bounding the number of equilibria of the electrostatic potential by those of the Euclidean distance function. We therefore wish to suggest a more nuanced formulation of the question inspired by a result about the heat-flow in [2]:

Is the L_1 -norm of the persistence diagram of V_p always smaller than that of V_q for any $1 \leq p \leq q$? In other words, does the combined “strength” of the equilibria monotonically decrease with shrinking parameter, p ?

Such decay in strength does not contradict the increase in number of equilibria, which can indeed happen, as shown by our counterexample. The main question of determining the maximum number of equilibria of an electrostatic potential defined by n point charges in \mathbb{R}^3 remains open.

²Indeed, for the weighted squared distance in (11), each point generates at most one interval along the line. This is not true for the weighted squared distance in (12), but it is not difficult to see that the point with minimum charge generates a single convex cell in three dimensions and therefore at most one interval along the line. The linear bound now follows by induction.

REFERENCES

- [1] F. AURENHAMMER AND H. EDELSBRUNNER. An optimal algorithm for constructing the weighted Voronoi diagram in the plane. *Pattern Recognition* **17** (1984), 251–257.
- [2] C. CHEN AND H. EDELSBRUNNER. Diffusion runs low on persistence fast. In “Proc. 13th Internat. Conf. Comput. Vision, 2011”, 423–430.
- [3] B. DELAUNAY. Sur la sphère vide. *Izv. Akad. Nauk SSSR, Otdelenie Matematicheskii i Estestvennykh Nauk* **7**, 1934, 793–800.
- [4] P. GAO AND M. R. DOUGLAS Geodesics on Calabi-Yau manifolds and winding states in non-linear sigma models. *Frontiers in Physics* **1**, 2013, 26.
- [5] H. EDELSBRUNNER AND J. PACH. Maximum Betti numbers of Čech complexes. In “Proc. 40th Internat. Sympos. Comput. Geom., 2024”, 53:1–53:14.
- [6] A. GABRIELOV, D. NOVIKOV AND B. SHAPIRO. Mystery of point charges. *Proc. London Math. Soc.* **95** (2007), 443–472.
- [7] J.C. MAXWELL. *A Treatise on Electricity and Magnetism, vol. 1*. Reproduction of 3-rd revised edition, Dover, New York, 1954.
- [8] P. MCMULLEN. On the upper-bound conjecture for convex polytopes. *J. Combinat. Theory, Ser. B* **10** (1971), 187–200.
- [9] J. MILNOR. *Morse Theory*. Princeton Univ. Press, Princeton, New Jersey, 1963.
- [10] M. MORSE AND S. CAIRNS. *Critical Point Theory in Global Analysis and Differential Topology*. Volume 33 in Pure and Applied Mathematics, Academic Press, New York and London, 1969.
- [11] A. OKABE, B. BOOTS, K. SUGIHARA AND S.N. CHIU. *Spatial Tessellations: Concepts and Applications of Voronoi Diagrams*. Second edition, Wiley, Hoboken, New Jersey, 2000.
- [12] G. OLIVEIRA Electrostatics and geodesics on $K3$ surfaces. *arXiv preprint* 2302.08354 2023.
- [13] G. VORONOI. Nouvelles applications des paramètres continus à la théorie des formes quadratiques. *J. Reine Angew. Math.* **133** (1907), 97–178 and **134** (1908), 198–287 and **136** (1909), 67–182.

APPENDIX A. ANALYTIC PROOF OF EXISTENCE OF EQUILIBRIA

This appendix illustrates how we can prove the existence of claimed equilibria. We shall do this for the cube; see the second row of Table 1, but the argument generalizes to the other Platonic solid with more electrostatic points beside the center, i.e. the dodecahedron.

Proposition 3. *The electrostatic potential defined by the (eight) unit point charges located at the vertices of a cube in \mathbb{R}^3 has twelve equilibria beside the one at the cube's center. These occur along the segments connecting the cube's center to the midpoints of its edges.*

Proof. Assume without loss of generality, that the vertices of the cube are located at the points $(\pm 1, \pm 1, \pm 1)$. The cube is invariant by a discrete group of symmetries, G , which contains, in particular, the reflections on the planes $P_1 = \{(x_1, x_2, x_3) \in \mathbb{R}^3 \mid x_2 = 0\}$ and $P_2 = \{(x_1, x_2, x_3) \in \mathbb{R}^3 \mid x_1 + x_3 = 0\}$. Denote these reflections $\sigma_1, \sigma_2: \mathbb{R}^3 \rightarrow \mathbb{R}^3$, respectively. Letting $v_1 = (0, 1, 0)$ and $v_2 = (1, 0, 1)$ be vectors orthogonal to these planes, the reflections change their signs: $\sigma_1(v_1) = -v_1$ and $\sigma_2(v_2) = -v_2$. Furthermore, the electrostatic potential V generated by unit charges at the vertices of this cube is invariant by these symmetries, i.e. $V \circ \sigma_1 = V \circ \sigma_2 = V$. Hence, we find from the symmetry that, along P_i ,

$$(13) \quad \langle \nabla V, v_i \rangle = \langle \sigma_i(\nabla V), \sigma_i(v_i) \rangle = -\langle \nabla V, v_i \rangle,$$

and therefore $\langle \nabla V, v_i \rangle = 0$, for $i = 1, 2$. In particular, along

$$(14) \quad P_1 \cap P_2 = \{(x_1, x_2, x_3) \in \mathbb{R}^3 \mid x_2 = 0, x_1 + x_3 = 0\}$$

$$(15) \quad = \{(x, 0, -x) \in \mathbb{R}^3 \mid x \in \mathbb{R}\}$$

we have $\langle \nabla V, v_1 \rangle = 0$ and $\langle \nabla V, v_2 \rangle = 0$, which we write more explicitly as

$$(16) \quad \frac{\partial V}{\partial x_2}(x, 0, -x) = \frac{\partial V}{\partial x_1}(x, 0, -x) + \frac{\partial V}{\partial x_3}(x, 0, -x) = 0.$$

We shall now prove the existence of an equilibrium of V by finding one in $P_1 \cap P_2$. Due to (16), we need only prove that there is an $x \in \mathbb{R}$ such that the function $f(x) = V(x, 0, -x)$ has a critical point, i.e. we must find x such that $f'(x) = 0$; that is:

$$(17) \quad \frac{\partial V}{\partial x_1}(x, 0, -x) - \frac{\partial V}{\partial x_3}(x, 0, -x) = 0.$$

The function $f'(x)$ is odd and varies continuously with x . We can explicitly compute it and therefore evaluate it at any point; see Figure 6. Evaluating the explicit formula for $f'(x)$ we find that

$$(18) \quad f'(-1) = \frac{8}{27} + \frac{8\sqrt{5}}{25} > 0,$$

$$(19) \quad f'(-1/2) = -\frac{4}{63} \left[\sqrt{7} \left(\sqrt{3} - \frac{27\sqrt{11}}{121} \right) - \frac{18}{7} \right] < 0,$$

$$(20) \quad f'(1/2) = \frac{4}{63} \left[\sqrt{7} \left(\sqrt{3} - \frac{27\sqrt{11}}{121} \right) - \frac{18}{7} \right] > 0,$$

$$(21) \quad f'(1) = \frac{8}{27} + \frac{8\sqrt{5}}{25} > 0.$$

We therefore conclude from the intermediate value theorem that there are two extra equilibria of V (zeroes of $f'(x)$) located at points $(x_*, 0, -x_*)$ and $(-x_*, 0, x_*)$ for $x_* \in (1/2, 1)$. Notice, in

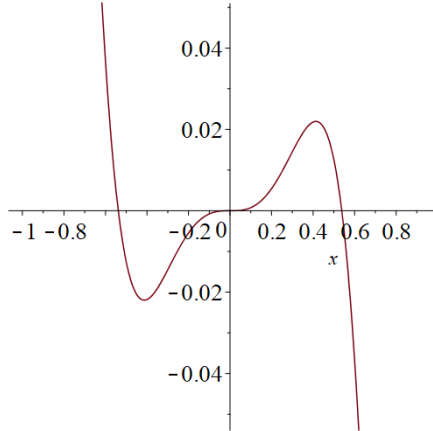


FIGURE 6. Plot of $f'(x)$ whose zeroes correspond to electrostatic points lying in the line $P_1 \cap P_2$.

particular, that such points lie along the straight lines passing through the cube's center and the midpoints in its edges.

These two points are in the same orbit of the group of symmetries of the cube and this orbit has cardinality 12 thus resulting in such a number of extra equilibria. \square

APPENDIX B. ARCHIMEDEAN AND CATALAN SOLIDS

In this appendix, we list the numbers of equilibria of the electrostatic potentials generated by placing unit point charges at the vertices of Archimedean and Catalan solids. We recall that an *Archimedean solid* is a convex polytope that is neither a Platonic solid nor a prism or anti-prism such that

- all facets are regular polygons;
- all vertices have the same local shape.

Conventionally, there are 13 Archimedean solids, but depending on the interpretation of the second condition, there may be a 14-th. In particular, we may or may not require vertex-transitivity (for any two vertices, there is a symmetry that maps one vertex into the other), which holds for the 13 Archimedean solids but not for the Elongated Square Gyrobicupola. The latter is similar to the Rhombicuboctahedron but has one of the square cuppola rotated by 45° relative to the opposite cupola; see Figure 7. Comparing rows 5 and 14 in Table 3, we see that the Elongated Square Gyrobicupola generates fewer equilibria than the Rhombicuboctahedron.

The *Catalan solids* are dual to the Archimedean solids, so the vertices have regular local shapes, and the facets are congruent to each other. There are again 13 classical examples, and the Pseudo Deltoidal Icositegrahedron as a 14-th solid that is not facet-transitive. Comparing rows 5 and 14 in Table 4, we see that the Pseudo Deltoidal Icositegrahedron generates again fewer equilibria than the similar Deltoidal Icositetrahedron.

Finally, we note that all Archimedean solids define electrostatic potentials with a positive number of (non-degenerate) 1-saddles, while all Catalan solids generate no such 1-saddles; compare Tables 3 and 4. Curiously, also the Platonic solids generate no 1-saddles; see Table 1. At this time, the authors of this paper have no explanation for this curious observation.

solid	f -vector	2-saddles	1-saddles	center
Truncated Tetrahedron	(12,18,8,1)	18	4	-3
Cuboctahedron	(12,24,14,1)	24	8	-5
Truncated Cube	(24,36,14,1)	36	8	-5
Truncated Octahedron	(24,36,14,1)	36	18	5
Rhombicuboctahedron	(24,48,26,1)	36	8	-5
Truncated Cuboctahedron	(48,72,26,1)	72	20	-5
Snub Cube	(24,60,38,1)	36	8	-5
Icosidodecahedron	(30,60,32,1)	60	20	-11
Truncated Dodecahedron	(60,90,32,1)	90	20	-11
Truncated Icosahedron	(60,90,32,1)	90	12	-19
Rhombicosidodecahedron	(60,120,62,1)	90	20	-11
Truncated Icosidodecahedron	(120,180,62,1)	180	50	-11
Snub Dodecahedron	(60,150,92,1)	90	20	-11
Elongated Square Gyrobicupola	(24,48,26,1)	32	8	-1

TABLE 3. The equilibria of the electrostatic potential of point charges at the vertices of the thirteen Archimedean solids and the Elongated Square Gyrobicupola. The f -vector gives the number of vertices, edges, facets, and the solid itself, in this sequence. Except possibly in the last case, the center is a degenerate equilibrium, and in each case, the number of 1-saddles is non-zero; compare with Table 4.

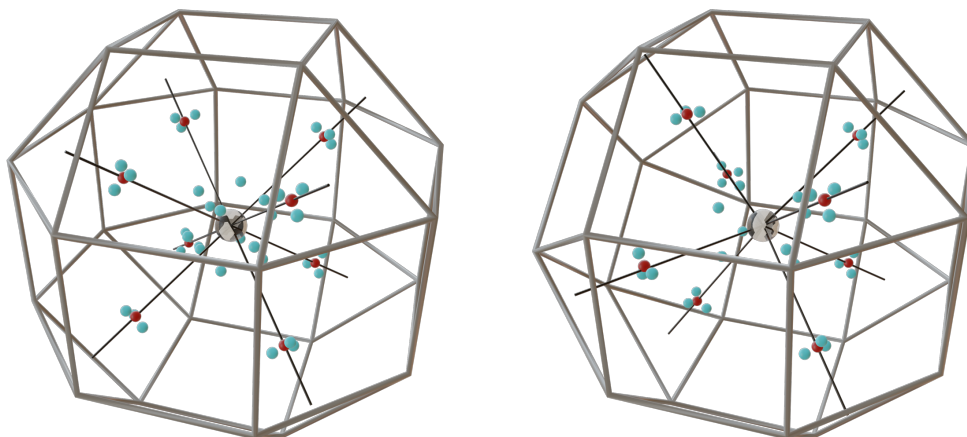


FIGURE 7. *Left*: the Rhombicuboctahedron and the equilibria of the electrostatic potential generated by unit point charges at its vertices. There are 36 *light blue* 2-saddles, 8 *dark red* 1-saddles, and a degenerate equilibrium at the center. *Right*: the Elongated Square Gyrobicupola—which differs from the Rhombicuboctahedron by the left cupola being rotated by 45° —and the equilibria of the electrostatic potential generated by unit point charges at its vertices. There are fewer equilibria: 32 *light blue* 2-saddles, 8 *dark red* 1-saddles, and a degenerate equilibrium at the center.

APPENDIX C. PRISMS AND ANTI-PRISMS

In this appendix, we provide details about the equilibria of the electrostatic potential for unit point charges placed at the vertices of regular prisms and anti-prisms. After introducing the building blocks of the analysis, we focus on the square and triangular anti-prisms.

C.1. Regular polygons. Let V_0 be the electric potential generated by unit point charges located at the vertices of a regular N -gon centered at the origin, $0 \in \mathbb{R}^3$, and placed on the horizontal plane spanned by the first two coordinate vectors. Denote by R the radius of the circle that passes through its vertices, and by $\alpha = \frac{2\pi}{N}$ the smallest angle that is a rotation symmetry of the N -gon.

solid	f -vector	2-saddles	1-saddles	center
Triakis Tetrahedron	(8,18,12,1)	10	0	-3
Rhombic Dodecahedron	(14,24,12,1)	18	0	-5
Triakis Octahedron	(14,36,24,1)	18	0	-5
Tetrakis Hexahedron	(14,36,24,1)	20	0	-7
Deltoidal Icositetrahedron	(26,48,24,1)	30	0	-5
Disdyakis Dodecahedron	(26,72,48,1)	30	0	-5
Pentagonal Icositetrahedron	(38,60,24,1)	48	0	-11
Rhombic Triacantahedron	(32,60,30,1)	42	0	-11
Triakis Icosahedron	(32,90,60,1)	42	0	-11
Pentakis Dodecahedron	(32,90,60,1)	50	0	-19
Deltoidal Hexecontahedron	(62,120,60,1)	72	0	-11
Disdyakis Triacantahedron	(62,180,120,1)	72	0	-11
Pentagonal Hexecontahedron	(92,150,60,1)	102	0	-11
Pseudo Deltoidal Icositetrahedron	(26,48,24,1)	26	0	-1

TABLE 4. The equilibria of the electrostatic potential of point charges at the vertices of the thirteen Catalan solids and the Pseudo Deltoidal Icositetrahedron. The f -vector gives the number of vertices, edges, facets, and the solid itself, in this sequence. Except possibly in the last case, the center is a degenerate equilibrium, and in each case, the number of 1-saddles vanishes; compare with Table 3.

We start by proving that the partial derivatives are symmetric with respect to the horizontal plane, and they all vanish at the origin.

Lemma 2. *Let $V_0: \mathbb{R}^3 \rightarrow \mathbb{R}$ be the electrostatic potential of unit point charges at the vertices of a regular N -gon, as described, and write $x = (x_1, x_2, x_3)$ for a point with its Cartesian coordinates in \mathbb{R}^3 . Then*

$$(22) \quad \frac{\partial V_0}{\partial x_3}(x_1, x_2, x_3) = -\frac{\partial V_0}{\partial x_3}(x_1, x_2, -x_3) \text{ and } \frac{\partial V_0}{\partial x_1}(0, 0, x_3) = \frac{\partial V_0}{\partial x_2}(0, 0, x_3) = 0.$$

Proof. The configuration is invariant by reflection through the $x_3 = 0$ plane, which contains the N -gon. Hence, $V_0(x_1, x_2, x_3) = V_0(x_1, x_2, -x_3)$ and differentiating with respect to x_3 gives the first relation. To see the second relation, note that the invariance of the N -gon under rotations of the horizontal plane by an angle α implies

$$(23) \quad V_0(x_1, x_2, x_3) = V_0(x_1 \cos \alpha + x_2 \sin \alpha, -x_1 \sin \alpha + x_2 \cos \alpha, x_3),$$

for all $x = (x_1, x_2, x_3) \in \mathbb{R}^3$. Differentiating with respect to x_1 and x_2 , respectively, and evaluating at $x_1 = x_2 = 0$ yields

$$(24) \quad \frac{\partial V_0}{\partial x_1}(0, 0, x_3) = \cos \alpha \frac{\partial V_0}{\partial x_1}(0, 0, x_3) - \sin \alpha \frac{\partial V_0}{\partial x_2}(0, 0, x_3);$$

$$(25) \quad \frac{\partial V_0}{\partial x_2}(0, 0, x_3) = \sin \alpha \frac{\partial V_0}{\partial x_1}(0, 0, x_3) + \cos \alpha \frac{\partial V_0}{\partial x_2}(0, 0, x_3).$$

This gives a system of linear equations for $\frac{\partial V_0}{\partial x_1}(0, 0, x_3)$ and $\frac{\partial V_0}{\partial x_2}(0, 0, x_3)$ whose only solution is when both vanish, as claimed. \square

It will also be useful to have the second partial derivative at the origin in vertical direction.

Lemma 3. For $V_0: \mathbb{R}^3 \rightarrow \mathbb{R}$ as before and all $x_3 \in \mathbb{R}$, we have

$$(26) \quad \frac{\partial^2 V_0}{(\partial x_3)^2}(0, 0, x_3) = -\frac{N}{(R^2 + x_3^2)^{5/2}} (R^2 - 2x_3^2).$$

Proof. Denote the vertices of the N -gon by $A_i = (a_{i,1}, a_{i,2}, 0)$, for $i = 1, 2, \dots, N$, and write r_i for the distance of A_i from a point $x = (x_1, x_2, x_3)$. Then the first and second partial derivatives along the vertical direction are

$$(27) \quad \frac{\partial V_0}{\partial x_3} = -\sum_{i=1}^N \frac{1}{r_i^2} \frac{\partial r_i}{\partial x_3} = -\sum_{i=1}^N \frac{x_3}{r_i^3};$$

$$(28) \quad \frac{\partial^2 V_0}{(\partial x_3)^2} = -\sum_{i=1}^N \left(\frac{1}{r_i^3} - 3\frac{x_3}{r_i^4} \frac{\partial r_i}{\partial x_3} \right) = -\sum_{i=1}^N \left(\frac{1}{r_i^3} - 3\frac{x_3^2}{r_i^5} \right) = -\sum_{i=1}^N \frac{1}{r_i^5} (r_i^2 - 3x_3^2).$$

Evaluating the second partial derivative at $(0, 0, x_3)$, we have $r_i^2 = R^2 + x_3^2$ independent of i , which implies (26). \square

C.2. Rotated prisms. We get a prism by connecting a regular N -gon with a copy of itself translated in an orthogonal direction. If we first rotate the copy by an angle β —around its center and within its plane—we call the convex hull of the two N -gons a β -rotated prism. For $\beta = \frac{\pi}{2}$, this is an anti-prism. Its *axis* is the line that passes through the centers of the two N -gons, its *radius* is the distance of the vertices from this line, and its *height* is the distance between the planes that contain the two N -gons. We now consider the electrostatic potential obtained by placing unit point charges at the vertices of such a β -rotated prism. Supposing the N -gons lie in horizontal planes at distance $\frac{h}{2}$ above and below the origin, the electrostatic potential is

$$(29) \quad \begin{aligned} V(x_1, x_2, x_3) &= V_0(x_1, x_2, x_3 + \frac{h}{2}) \\ &+ V_0(x_1 \cos \beta + x_2 \sin \beta, -x_1 \sin \beta + x_2 \cos \beta, x_3 - \frac{h}{2}). \end{aligned}$$

Not surprisingly, the type of the equilibrium at the origin depends on the height, but with the exception of a particular height, it does not depend on the angle of the rotation.

Theorem 3. Let $\beta \in \mathbb{R}/2\pi\mathbb{Z}$, $R > 0$, and $h > 0$. Consider the electrostatic potential generated by unit point charges at the vertices of a β -rotated prism with radius R and height h . Then, its center is a non-degenerate equilibrium iff $h \neq \sqrt{2}R$, in which case the center is a 1-saddle if $h < \sqrt{2}R$ and a 2-saddle if $h > \sqrt{2}R$. Moreover, in the latter case there are two additional 1-saddles along the axis of the β -rotated prism.

Proof. To use the form of the potential in (29), we assume that the two N -gons of the β -rotated prism lie in horizontal planes and its center is the origin in \mathbb{R}^3 . We start by confirming that the origin is always an equilibrium. Using Lemma 2, we obtain

$$(30) \quad \frac{\partial V}{\partial x_i}(0, 0, 0) = \frac{\partial V_0}{\partial x_i}(0, 0, \frac{h}{2}) + \frac{\partial V_0}{\partial x_i}(0, 0, -\frac{h}{2}) = 0,$$

which for $i = 1, 2$ is true because both partial derivatives vanish, and for $i = 3$ follows from the symmetry across the horizontal coordinate plane. Next we investigate the Hessian at the origin. By differentiating the identity $\frac{\partial V_0}{\partial x_3}(x_1, x_2, x_3) = -\frac{\partial V_0}{\partial x_3}(x_1, x_2, -x_3)$ with respect to x_1, x_2 , and x_3 ,

we obtain

$$(31) \quad \frac{\partial^2 V_0}{\partial x_i \partial x_3}(x_1, x_2, x_3) = -\frac{\partial^2 V_0}{\partial x_i \partial x_3}(x_1, x_2, -x_3);$$

$$(32) \quad \frac{\partial^2 V_0}{(\partial x_3)^2}(x_1, x_2, x_3) = \frac{\partial^2 V_0}{(\partial x_3)^2}(x_1, x_2, -x_3),$$

for $i = 1, 2$. Hence, using the first of these identities, we have

$$(33) \quad \frac{\partial^2 V}{\partial x_i \partial x_3}(0, 0, 0) = \frac{\partial^2 V_0}{\partial x_i \partial x_3}(0, 0, \frac{h}{2}) + \frac{\partial^2 V_0}{\partial x_i \partial x_3}(0, 0, -\frac{h}{2}) = 0.$$

This shows that $\lambda_3 = \frac{\partial^2 V}{(\partial x_3)^2}(0, 0, 0)$ is an eigenvalue of the Hessian at the origin. Using the second identity above, we see that this eigenvalue satisfies

$$(34) \quad \lambda_3 = \frac{\partial^2 V}{(\partial x_3)^2}(0, 0, 0) = \frac{\partial^2 V_0}{\partial x_i \partial x_3}(0, 0, \frac{h}{2}) + \frac{\partial^2 V_0}{\partial x_i \partial x_3}(0, 0, -\frac{h}{2}) = 2 \frac{\partial^2 V_0}{(\partial x_3)^2}(0, 0, \frac{h}{2}).$$

The rotational symmetry by $\beta \neq 0$ then implies that the remaining two eigenvalues must coincide: $\lambda_1 = \lambda_2 = \lambda$. Furthermore, since V is harmonic, we have $\lambda = -\frac{\partial^2 V_0}{(\partial x_3)^2}(0, 0, \frac{h}{2})$. It remains to compute this quantity and show it vanishes precisely when $h = \sqrt{2}R$ as claimed in the statement. This can be done by making use of Lemma 3 to obtain

$$(35) \quad \frac{\partial^2 V}{(\partial x_3)^2}(0, 0, 0) = -\frac{2N}{(R^2 + x_3^2)^{5/2}} \left(R^2 - \frac{h^2}{2} \right),$$

which vanishes iff $h = \sqrt{2}R$. Furthermore, the eigenvalues of the Hessian at the origin are

$$(36) \quad \lambda_3 = -\frac{2N}{(R^2 + x_3^2)^{5/2}} \left(R^2 - \frac{h^2}{2} \right);$$

$$(37) \quad \lambda_1 = \lambda_2 = \frac{N}{(R^2 + x_3^2)^{5/2}} \left(R^2 - \frac{h^2}{2} \right).$$

We therefore conclude that for $h < \sqrt{2}R$ we have $\lambda_1 = \lambda_2 > 0$ and $\lambda_3 < 0$, so the origin is a 1-saddle. On the other hand, if $h > \sqrt{2}R$ we have $\lambda_1 = \lambda_2 < 0$ and $\lambda_3 > 0$, and so the origin is a 2-saddle. However, in this case there are at least two additional equilibria along the axis of the β -rotated prism, which by construction is the x_3 -axis. To prove their existences, we compute the derivatives of V along this axis:

$$(38) \quad \frac{\partial V}{\partial x_i}(0, 0, x_3) = \frac{\partial V_0}{\partial x_i}(0, 0, x_3 + \frac{h}{2}) + \frac{\partial V_0}{\partial x_i}(0, 0, x_3 - \frac{h}{2}) = 0 + 0 = 0,$$

for $i = 1, 2$. Hence, we need only look for zeroes of $\frac{\partial V}{\partial x_3}(0, 0, x_3)$, which we compute as

$$(39) \quad \frac{\partial V}{\partial x_3}(0, 0, x_3) = \frac{\partial V_0}{\partial x_3}(0, 0, x_3 + \frac{h}{2}) + \frac{\partial V_0}{\partial x_3}(0, 0, x_3 - \frac{h}{2}).$$

To compute the two terms on the right-hand side, we use Lemma 3 and find that $\frac{\partial V_0}{\partial x_3} = -\sum_{i=1}^N \frac{x_3}{r_i^3}$, where $r_i(x_1, x_2, x_3)^2 = (x_1 + a_{i1})^2 + (x_2 - a_{i2})^2 + x_3^2$. From this it follows that

$$(40) \quad \frac{\partial V}{\partial x_3}(0, 0, x_3) = -\sum_{i=1}^N \frac{x_3 + \frac{h}{2}}{r_i^3(0, 0, x_3 + \frac{h}{2})} - \sum_{i=1}^N \frac{x_3 - \frac{h}{2}}{r_i^3(0, 0, x_3 - \frac{h}{2})}$$

$$(41) \quad = -N \frac{x_3 + \frac{h}{2}}{(R^2 + (x_3 + \frac{h}{2})^2)^{3/2}} - N \frac{x_3 - \frac{h}{2}}{(R^2 + (x_3 - \frac{h}{2})^2)^{3/2}}.$$

Evaluating this at the top and bottom of the β -rotated prism, we obtain

$$(42) \quad \frac{\partial V}{\partial x_3}(0, 0, \frac{h}{2}) = -\frac{h}{(R^2 + h^2)^{3/2}} < 0 \text{ and } \frac{\partial V}{\partial x_3}(0, 0, -\frac{h}{2}) = \frac{h}{(R^2 + h^2)^{3/2}} > 0.$$

On the other hand, further differentiating with respect to x_3 , as in the proof of Theorem 3, we find that

$$(43) \quad \frac{\partial^2 V}{\partial x_3^2}(0, 0, 0) = -\frac{2N}{(R^2 + x_3^2)^{5/2}} \left(R^2 - \frac{h^2}{2}\right),$$

which is positive when $h > \sqrt{2}R$. Hence, there exists $\varepsilon > 0$, such that $\frac{\partial V}{\partial x_3}(0, 0, t)$ is positive for $t \in (0, \varepsilon)$ and negative for $t \in (-\varepsilon, 0)$. Combining this with the previously computed values of $\frac{\partial V}{\partial x_3}$ at the centers of the two N -gons, the intermediate value theorem implies that $\frac{\partial V}{\partial x_3}$ has two additional zeroes along the x_3 -axis.

We now characterize these equilibria by showing that they are 1-saddles. At both, $V(0, 0, x_3)$ increases on the left and decreases on the right, so they are local maxima of the potential restricted to the x_3 -axis. Given that the potential is harmonic, at least one of the remaining eigenvalues of the Hessian must be positive, and by rotational symmetry so must the other. As the Hessian has a single negative eigenvalue, both equilibria are 1-saddles. \square

C.3. The square anti-prism. We shall now conduct a more thorough study of the square anti-prism. For concreteness, let $A_1 = (1, 0, \frac{h}{2})$, $A_2 = (0, 1, \frac{h}{2})$, $A_3 = (-1, 0, \frac{h}{2})$, $A_4 = (0, -1, \frac{h}{2})$ be the vertices of the square at the top, and $B_1 = (\frac{\sqrt{2}}{2}, \frac{\sqrt{2}}{2}, -\frac{h}{2})$, $B_2 = (-\frac{\sqrt{2}}{2}, \frac{\sqrt{2}}{2}, -\frac{h}{2})$, $B_3 = (-\frac{\sqrt{2}}{2}, -\frac{\sqrt{2}}{2}, -\frac{h}{2})$, $B_4 = (\frac{\sqrt{2}}{2}, -\frac{\sqrt{2}}{2}, -\frac{h}{2})$ the vertices of the square at the bottom. Hence, the origin of \mathbb{R}^3 is the center, the x_3 -axis is the axis, $R = 1$ is the radius, and h is the height of the anti-prism. Its *lateral* edges are the ones that connect vertices of the two squares.

Proposition 4. *For $h < \sqrt{2}R$, there is an equilibrium on the segment connecting the center of the square anti-prism to the midpoint of every lateral edge.*

Proof. Consider the open half-lines that emanate from the origin and pass through the midpoints of the lateral edges of the anti-prism. There is no loss of generality in only considering one of these, namely the one that maps $t > 0$ to $L(t) = \frac{t}{2}(A_1 + B_1) = \frac{t}{4}(2 + \sqrt{2}, \sqrt{2}, 0)$, with normal vectors $n_1 = (0, 0, 1)$ and $n_2 = (-\sqrt{2}, 2 + \sqrt{2}, 0)$. Then, by direct computation, we find that along L the

directional derivatives both vanish:

$$(44) \quad \langle n_1, \nabla V(L(t)) \rangle = \frac{\partial V}{\partial x_3}(L(t)) = 0,$$

$$(45) \quad \langle n_2, \nabla V(L(t)) \rangle = -\sqrt{2} \frac{\partial V}{\partial x_1}(L(t)) + (2 + \sqrt{2}) \frac{\partial V}{\partial x_2}(L(t)) = 0.$$

Therefore, along L , the gradient ∇V is parallel to it, and

$$(46) \quad \langle \dot{L}(t), \nabla V(L(t)) \rangle = \frac{2 + \sqrt{2}}{4} \frac{\partial V}{\partial x_1}(L(t)) + \frac{\sqrt{2}}{4} \frac{\partial V}{\partial x_2}(L(t)),$$

which we can also compute explicitly but has a very long and not very enlightening expression. Instead, notice that this quantity vanishes when $t = 0$ and its first derivative at this point is

$$(47) \quad \left. \frac{d}{dt} \right|_{t=0} \langle \dot{L}(t), \nabla V(L(t)) \rangle = 16 \frac{2\sqrt{2} + 5}{(h^2 + 4)^{5/2}} (2 - h^2),$$

which is positive if $h < \sqrt{2}R$. In particular, there is $\varepsilon > 0$ such that this function is positive for $t \in (0, \varepsilon)$ and negative for $t \in (-\varepsilon, 0)$. On the other hand, evaluating this function at $t = \pm 1$, we find $\langle \dot{L}(-1), \nabla V(L(-1)) \rangle > 0$ and $\langle \dot{L}(1), \nabla V(L(1)) \rangle < 0$. By the intermediate value theorem, there must be two extra zeroes along this line. \square

For $h = \sqrt{2}R$, the complexity of the degenerate equilibrium at the origin is encapsulated by the Taylor expansion of the potential at the origin in homogeneous harmonic polynomials. As we shall see, not only the degree-2 terms vanish,³ but also the degree-3 terms do.

Lemma 4. *Let $V: \mathbb{R}^3 \rightarrow \mathbb{R}$ be the electrostatic potential generated by unit point charges placed at the vertices of the square anti-prism as specified at the beginning of this subsection. For $h = \sqrt{2}R$, its Taylor series at the origin is given by*

$$(48) \quad V(x_1, x_2, x_3) = \frac{8\sqrt{6}}{3} \left(1 - \frac{7}{108}(x_1^4 + x_2^4) - \frac{14}{81}x_3^4 - \frac{7}{54}x_1^2x_2^2 + \frac{14}{27}x_3^2(x_1^2 + x_2^2) \right) + \dots,$$

with terms of order exceeding 4 not shown.

C.4. The triangular anti-prism. We now turn to the case of the triangular anti-prism, using the geometric realization in which the vertices at the top are $A_1 = (\sqrt{3}, 1, \frac{h}{2})$, $A_2 = (-\sqrt{3}, 1, \frac{h}{2})$, $A_3 = (0, -2, \frac{h}{2})$, and those at the bottom are $B_1 = (\sqrt{3}, -1, -\frac{h}{2})$, $B_2 = (0, 2, -\frac{h}{2})$, $B_3 = (-\sqrt{3}, -1, -\frac{h}{2})$. Hence, $0 \in \mathbb{R}^3$ is the center, the x_3 -axis is the axis, $R = 2$ is the radius, and h is the height of the anti-prism. We start with a result analogous to the proposition we proved for the square anti-prism.

Proposition 5. *For $h < \sqrt{2}R$, there is an equilibrium on the open half-line connecting the center of the triangular anti-prism to the midpoint of every lateral edge.*

Proof. Without loss of generality, we can consider the lateral edge connecting A_1 and B_1 . Its midpoint is $\frac{1}{2}(A_1 + B_1) = (\sqrt{3}, 0, 0)$, so the half-line connecting the origin to this point is the positive half of the x_1 -axis. We parametrize it by $L(t) = t(\sqrt{3}, 0, 0)$ and note that it has normal vectors $n_1 = (0, 1, 0)$ and $n_2 = (0, 0, 1)$. Computing the derivatives in the direction of n_1 and n_2

³We already knew this from the vanishing of the Hessian in the proof of Theorem 3.

along this line, we find that both vanish:

$$(49) \quad \langle \nabla V(L(t)), n_1 \rangle = \frac{\partial V}{\partial x_2}(L(t)) = 0 \text{ and } \langle \nabla V(L(t)), n_2 \rangle = \frac{\partial V}{\partial x_3}(L(t)) = 0.$$

The remaining directional derivative along $\dot{L}(t) = (\sqrt{3}, 0, 0)$ is

$$(50) \quad \langle \dot{L}(t), \nabla V(L(t)) \rangle = \sqrt{3} \frac{\partial V}{\partial x_1}(L(t))$$

$$(51) \quad = -2\sqrt{3} \frac{t+1}{\left(3(t+1)^2 + 1 + \frac{h^2}{4}\right)^{3/2}} - 2\sqrt{3} \frac{t-1}{\left(3(t-1)^2 + 1 + \frac{h^2}{4}\right)^{3/2}}$$

$$(52) \quad - 16\sqrt{3} \frac{t}{(12t^2 + 16 + h^2)^{3/2}},$$

and the derivative of this quantity at $t = 0$ is given by $48\sqrt{3} \frac{8-h^2}{(h^2+16)^{5/2}}$, which is positive if $h < 2\sqrt{2} = \sqrt{2}R$ and so it is positive for small positive t . On the other hand, we have

$$(53) \quad \sqrt{3} \frac{\partial V}{\partial x_1}(L(1)) = -\frac{4\sqrt{3}}{\left(13 + \frac{h^2}{4}\right)^{3/2}} - \frac{16\sqrt{3}}{(h^2 + 28)^{3/2}} < 0,$$

so it must have a zero in the interval $(0, 1)$ corresponding to an equilibrium. \square

Again we compute the Taylor expansion at the origin as a way to understand the degenerate critical point there for $h = \sqrt{2}R$.

Lemma 5. *Let $V: \mathbb{R}^3 \rightarrow \mathbb{R}$ be the electrostatic potential generated by unit point charges placed at the vertices of the triangular anti-prism as specified at the beginning of this subsection. For $h = \sqrt{2}R$, its Taylor series at the origin is given by*

$$(54) \quad \sqrt{3} - \frac{7\sqrt{3}}{216} \left(\frac{x_1^4}{8} + \frac{x_2^4}{8} + \frac{x_3^2}{3} + \frac{x_1^2 x_2^2}{4} - x_1^2 x_3^2 - x_2^2 x_3^2 + \frac{5\sqrt{2}}{2} x_2 x_3 (x_2^2 - x_1^2) \right) + \dots,$$

with terms of order exceeding 4 not shown.

APPENDIX D. PROOFS OF PROPOSITIONS 1 AND 2

We first prove that, when $p \geq 1$, the function $V_p: \mathbb{R}^3 \setminus \{A_1, A_2, \dots, A_n\} \rightarrow \mathbb{R}$ defined in (9) has no local maxima if all charges are positive.

Proof of Proposition 1. The case $p = 1$ follows immediately from the fact that $V_1 = V$ is harmonic. Hence, it suffices to consider the case $p > 1$. For this, we show that the Laplacian satisfies $\Delta V_p > 0$. Since it is the trace of the Hessian and thus the sum the diagonal eigenvalues, there must be at least one positive eigenvalue, which is incompatible with the existence of a maximum. To carry out the computation of ΔV_p , we write $r_i(x) = \|x - A_i\|$ and thus $V_p(x) = \sum_{i=1}^n \zeta_i^p / r_i(x)^p$. Let x_1, x_2, x_3

be the coordinates in \mathbb{R}^3 and $A_i = (a_{i1}, a_{i2}, a_{i3})$. Then, using $\frac{\partial r_i}{\partial x_j}(x) = \frac{x_j - a_{ij}}{r_i}$, we compute

$$(55) \quad \frac{\partial V_p}{\partial x_j} = -p \sum_{i=1}^n \frac{\zeta_i^p}{r_i^{p+1}} \frac{\partial r_i}{\partial x_j} = -p \sum_{i=1}^n \frac{\zeta_i^p}{r_i^{p+2}} (x_j - a_{ij});$$

$$(56) \quad \frac{\partial^2 V_p}{\partial x_j^2} = -p \sum_{i=1}^n \zeta_i^p \left(\frac{1}{r_i^{p+2}} - (p+2) \frac{x_j - a_{ij}}{r_i^{p+3}} \frac{\partial r_i}{\partial x_j} \right)$$

$$(57) \quad = -p \sum_{i=1}^n \zeta_i^p \left(\frac{1}{r_i^{p+2}} - (p+2) \frac{(x_j - a_{ij})^2}{r_i^{p+4}} \right)$$

$$(58) \quad = -p \sum_{i=1}^n \frac{\zeta_i^p}{r_i^{p+2}} \left(1 - (p+2) \frac{(x_j - a_{ij})^2}{r_i^2} \right).$$

Finally, summing over the three coordinate directions, we find that

$$(59) \quad \Delta V_p = \sum_{j=1}^3 \frac{\partial^2 V_p}{\partial x_j^2} = -p \sum_{i=1}^n \frac{\zeta_i^p}{r_i^{p+2}} \left(3 - (p+2) \sum_{j=1}^3 \frac{(x_j - a_{ij})^2}{r_i^2} \right)$$

$$(60) \quad = -p \sum_{i=1}^n \frac{\zeta_i^p}{r_i^{p+2}} (3 - (p+2)) = p(p-1) \sum_{i=1}^n \frac{\zeta_i^p}{r_i^{p+2}},$$

which is positive if all ζ_i are positive. \square

Remark 1. *If one trades the assumption that $p \geq 1$ for $p \leq 1$ we can actually conclude, from the same proof, that there are no maxima. On the other hand, if one continues to assume that $p \geq 1$, but that instead that all ζ_i^p are negative, then the same proof shows that there are no minima when $p \geq 1$. These conclusions are particular cases of the following more general statement which can be inferred from the same proof. Suppose that $p > 0$, then:*

- if $(p-1)\zeta_i^p > 0$ for all $i \in \{1, 2, \dots, n\}$, then there are no local maxima;
- if $p = 1$, then there are neither local minima nor minima;
- if $(p-1)\zeta_i^p < 0$ for all $i \in \{1, 2, \dots, n\}$, then there are no local minima.

Next, we shall prove that for $p > 1$ the potentials V_p can have minima when all the charges are positive. This will be done by exploring the example given by placing the charges at the vertices of an octahedron.

Proof of Proposition 2. With no loss of generality, we can choose the vertices of the octahedron at the points $(\pm 1, 0, 0)$, $(0, \pm 1, 0)$, $(0, 0, \pm 1)$, in which case the center of the octahedron coincides with the origin, $(0, 0, 0)$. Then, using the computations carried out in the proof of Proposition 1, we find that

$$(61) \quad \frac{\partial^2 V_p}{\partial x_i \partial x_j}(0, 0, 0) = 0,$$

$$(62) \quad \frac{\partial^2 V_p}{\partial x_i^2}(0, 0, 0) = 2p(p-1),$$

for $i \neq j$ and $i \in \{1, 2, 3\}$, respectively. Hence, the Hessian of V_p at the origin is positive definite whenever $p > 1$ and the result follows. \square

ISTA (INSTITUTE OF SCIENCE AND TECHNOLOGY AUSTRIA), KLOSTERNEUBURG, AUSTRIA
Email address: `Herbert.Edelsbrunner@ista.ac.at`

ISTA (INSTITUTE OF SCIENCE AND TECHNOLOGY AUSTRIA), KLOSTERNEUBURG, AUSTRIA
Email address: `cdfillmore@gmail.com`

IST (INSTITUTO SUPERIOR TÉCNICO), UNIVERSIDADE DE LISBOA, PORTUGAL
Email address: `galato97@gmail.com`